

Bone Texture Analysis on Direct Digital Radiographic Images: Precision Study and Relationship with Bone Mineral Density at the Os Calcis

E. Lespessailles,¹ C. Gadois,¹ G. Lemineur,² J. P. Do-Huu,² L. Benhamou¹

¹Institut de Prévention et de Recherche de l'Ostéoporose, Service de Rhumatologie CHR d'Orléans, 1 rue porte madeleine 4500 Orléans, France

²D3A Medical Systems, 16 rue leonard de vinci 45074 Orleans, France

Received: 9 August 2006 / Accepted: 23 October 2006 / Online publication: 2 February 2007

Abstract. Assessment of bone microarchitecture in complement to bone mineral density (BMD) exam could improve prediction of osteoporotic fractures. A high-resolution X-ray prototype was developed to assess microarchitecture quality. Images were obtained on os calcis; then, three texture parameters were calculated on the same region of interest (ROI): a fractal parameter, a run-length parameter, and a co-occurrence parameter. This work describes the reproducibility of this method. We also examine the relationship between texture parameters and BMD at a site-matched ROI. Measurements on the left heel were performed on 30 healthy women, on the same day, with repositioning for short-term precision error. An additional measurement was done at 1 week to evaluate mid-term precision error on 14 subjects. Os calcis images from 10 healthy women were used to evaluate both intra- and interobserver reproducibility. Thirty other healthy patients were measured successively on two similar devices for inter-prototype comparison. BMD and texture analyses of the left heel were obtained from 57 women. Short-term precision errors ranged 1.16–1.24% according to the texture parameter. Mid-term precision error was slightly higher than short-term precision for the mean Hurst exponent parameter. Comparisons of texture parameters and BMD at a site-matched ROI on the os calcis showed no significant relationships. The results also show that the use of this high-resolution digital X-ray device improves the reproducibility of parameter measurement compared to the indirect digitization of radiologic films previously used.

Key words: Osteoporosis — Texture analysis — Os calcis — Microarchitecture — Reproducibility

Osteoporosis (OP) is characterized by a decrease in the biomechanical competence of bone leading to fractures. Although the risk of OP fractures increases as bone mineral density (BMD) decreases, lower energy fractures in patients older than 50 years often come in women with osteopenia, as defined by the World Health

Organization [1]. Approximately one-half of all fractures occur among women without OP [2, 3]. Furthermore, it has been shown that there was an overlap in BMD measurements between controls and fracture patients, suggesting that BMD alone does not explain all heterogeneity in the pathogenesis of bone fragility in women with fractures [4]. Other bone properties play an important role in the mechanical properties of trabecular bone [5, 6]. Among them, trabecular bone microarchitecture is considered to have a central role and has been included as a part of the definition of OP [7]. Trabecular microarchitectural alterations (loss of trabecular plates and of their connection) produce greater deficit in bone strength than does trabecular thinning [8]. Recent imaging techniques produce three-dimensional (3D) images of trabecular bone [9]; however, their applicability to large populations may be limited by their cost and availability.

As a cheaper alternative, it has been shown that texture analysis of X-ray radiographs is well suited to assess changes in trabecular bone architecture [10, 11]. In addition, it has been shown that fractal analysis on conventional radiography provides additional information beyond BMD in correlating with biomechanical properties [12, 13]. We have found that fractal dimension measured on a 2D gray-level projection texture obtained from high-resolution 3D magnetic resonance imaging was significantly associated with porosity and connectivity [14]. Other authors have also found significant correlations between radiographic patterns and parameters measured either on micro-computed tomography (CT) [15] or on synchrotron [16]. As we have shown that a texture analysis was independent and complementary with BMD for determining the odd-ratio of fractures [17], it would be interesting to combine this analysis with BMD results and other factors that play independent roles in the prediction of fractures like the fracture index proposed by Black et al. [18].

The role of microarchitecture in the treatment of OP is obvious [19]. BMD and bone markers do not reflect

Correspondence to: E. Lespessailles; E-mail: eric.lespessailles@chr-orleans.fr

deterioration of trabecular architecture and do not accurately explain the preservation of bone microarchitecture obtained with bisphosphonates [20, 21] or its improvement observed with teriparatide [22]. It has been hypothesized that texture analysis may reflect significant treatment-related differences in trabecular bone microarchitecture [23].

We have previously validated trabecular bone texture analysis on radiographs and assessed its reproducibility [24]. Relationships of both histomorphometric [25] and biomechanical [26] properties with texture parameters have been shown. Then, we have determined its value to discriminate OP patients with bone fractures from controls [27]. However, this analysis required the use of very standardized procedures as well as obtaining radiographs to digitize the images. Assuming, firstly, that direct digitization of images would improve the reproducibility of our technique by reducing potential precision errors linked to digitization of radiographic films and, secondly, that the parameters measured by texture analysis are not merely surrogate markers of bone density, the aims of this study were (1) to assess the reproducibility of a texture analysis obtained with a new high-resolution digital X-ray prototype designed by our laboratory and (2) to compare the results of texture analysis parameters with BMD at the same region of interest (ROI).

Materials and Methods

Image Acquisition

Images were obtained on the os calcis with a direct digital X-ray prototype with the following characteristics. Focal distance was set at 1.15 m. The lateral part of the left heel was placed in contact with the sensor. X-ray parameters were set at 55 kV and 20 mAs. The high-resolution digital detector integrated with this prototype had a 50 μm pixel size, providing a spatial resolution of 8 lp/mm at 10% modulation transfer function. Scanning the heel permitted the selection of a similar measurement site (ROI) for each subject by using individual anatomical landmarks as previously described [24]. These anatomical landmarks are localized by the operator, allowing positioning of the ROI (1.6 \times 1.6 cm^2) performed by the software device (Fig. 1). Then, three texture parameters were calculated on the ROI to evaluate the bone microarchitectural quality.

Trabecular Bone Texture Parameters

H_{mean} parameter. The gray levels of the ROI were fitted to the most used fractal model for texture images: the fractional Brownian motion (fBm). In this case, fractal shapes are described by a single parameter, H (Hurst exponent), related to the fractal dimension, D, by $H = 2 - D$. The higher H is, the smaller the roughness of the path. However, due to its non-stationary nature, fBm is difficult to analyze directly. Therefore, we used the increments of fBm called fractional gaussian noise (fGn), which is a stationary process. The maximum likelihood estimator (MLE) was applied to the fGn to estimate H [28]. The estimation of the H_{mean} parameter is described in

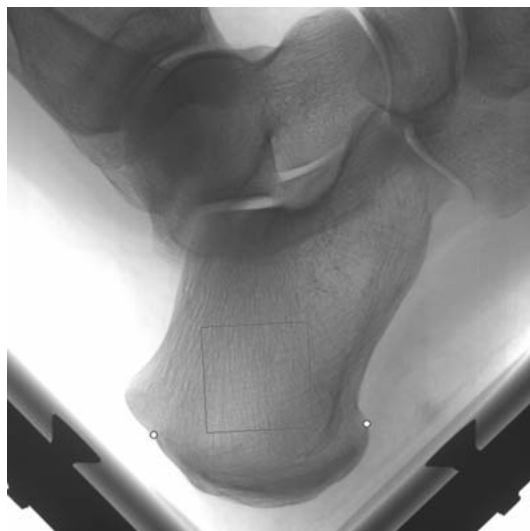


Fig. 1. ROI for texture analysis at the os calcis with anatomical landmarks.

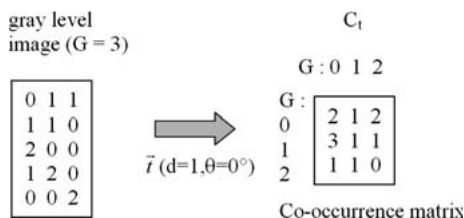


Fig. 2. Example of a run-length matrix in which rows represent the gray level of the run and columns represent the length of the run. One element, $RL_\theta(i, j)$, of this matrix indicates the number of runs with a gray level (i) and a length (j) found in the image in the direction θ .

detail elsewhere [24]. For an image, H was estimated on each parallel line in the direction under study. So, the H_{mean} of this direction was obtained by averaging all these values and the H_{mean} of the image was obtained by averaging 36 directions following 10° step of analysis [24].

Run-length parameter. A run is a set of consecutive pixels having the same gray-level value in a given direction [29–31]. A run-length matrix is a 2D array, RL, in which rows represent the gray level of the run and columns represent the length of the run. One element, $RL_\theta(i, j)$, of this matrix indicates the number of runs with a gray level (i) and a length (j) found in the image in the direction θ (Fig. 2). Run-length encoding is based on the extraction of texture parameters from the statistical repartition of runs. Many run-length parameters can be calculated; for this study, the short run emphasis parameter was chosen (see equation 1).

$$SR = \frac{1}{\sum_i \sum_j RL_\theta(i, j)} \sum_i \sum_j \frac{RL_\theta(i, j)}{j^2} \quad (1)$$

This parameter is expected to be large for fine textures [29].

Co-occurrence parameter. In this case, a co-occurrence matrix is a 2D array, C, in which both rows and columns represent a set of possible image values. $C_1(i, j)$ indicates how many times

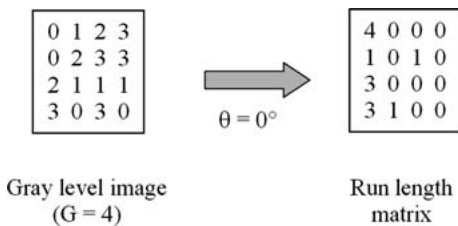


Fig. 3. Example of a co-occurrence matrix in which both rows and columns represent a set of possible image values. The matrix indicates how many times the gray-level value i co-occurs following a translation vector, $t = (d; \theta)$, with the gray-level value j ; d represents the distance between the two pixels and θ , the direction.

the gray level value (i) co-occurs following a translation vector, $t = (d, \theta)$, with the gray-level value j (Fig. 3); d represents the distance between the two pixels and θ , the direction. For this study, although many parameters of co-occurrence exist, we chose to estimate the energy parameter as defined by Haralick (eq. 2) [29]. Moreover, we computed d equal to 1.

$$\text{Energy} = \sum_{ij} N_{\theta}(i, j)^2 \quad (2)$$

Estimation of all these parameters was performed for eight directions, and then we calculated the mean values for all the images.

Quality control. A calibration test was carried out each day of exam using an external phantom to detect any potential drift of the instrumentation. Both image quality control and quantitative results were checked. Figure 4a shows a photograph of the phantom and Figure 4b, the corresponding digitized image. We did not observe any drift during the period of precision protocol.

Precision Protocol

The root-mean-square (RMS) coefficient of variation (CV) formula was used to calculate all reproducibility data [32].

- Short-term precision error ($S - CV$) was estimated using the CV, which is based on the calculation of the average RMS of the individual subject's Standard Deviation (SD_i) of repeated measurements at one time point, as recommended by Gluer et al. [9].
- Mid-term precision error ($M - CV$) was also estimated by the CV, based on calculation of the average RMS of the individual subject's SD (SD_i) of repeated measurements at three time points.
- Intraobserver reproducibility (IntraOR): one observer extracted the ROI three times on each image for 10 subjects.
- Interobserver reproducibility (InterOR): three observers extracted the ROI one time for each of 10 subjects.
- Interprototype comparison: 30 subjects were measured successively on two similar devices.
- *In vitro* reproducibility: 42 images performed over 2 consecutive days on the same os calcis phantom.

Subjects and Patients

This protocol was evaluated and approved by the Regional Ethics Committee (Tours, France).

Each subject or patient gave informed consent to enter this study.

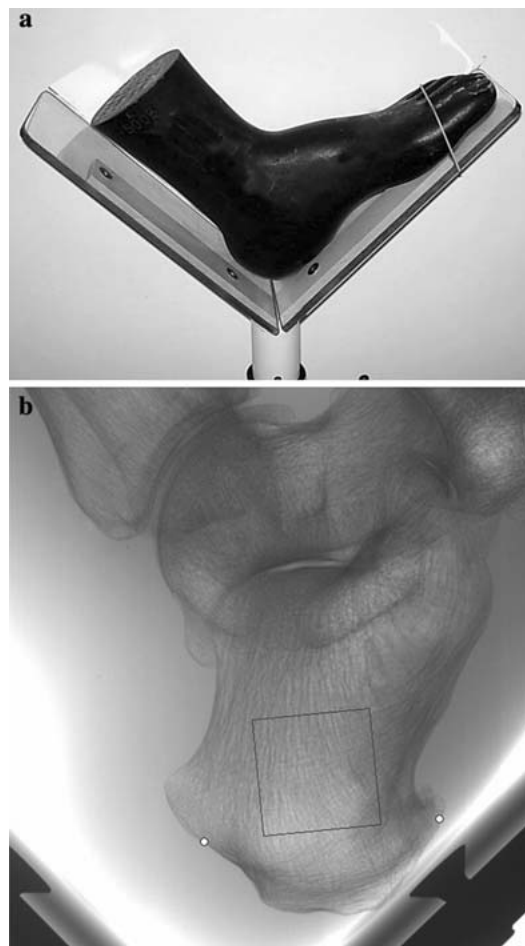


Fig. 4. (a) The phantom used for quality control and (b) its digitized image.

Thirty healthy women referred to our bone densitometry unit (58.2 ± 6.8 years of age) were measured twice on the left heel on the same day, with repositioning for short-term precision error. Fourteen subjects from our medical staff and research team (3 men, 11 women) aged 44.2 ± 14.4 years had three measurements at 1-week intervals (D0–D7–D14) to evaluate the mid-term precision error. Os calcis images from 10 healthy women were used to evaluate both intraOR and interOR. Thirty other healthy patients referred to our bone densitometry unit were measured successively on two similar devices for interprototype comparison.

The same observer (C. G.) extracted ROI for the reproducibility study *in vitro*, short-term, mid-term, and interprototype comparisons.

Influence of Foot Positioning

In order to have proper positioning, the foot has to be in contact at three points with the image sensor. One point concerns the leg, the second corresponds to the ankle, the third is at the fifth toe (Fig. 5). In the first step, we analyzed the foot phantom in the proper position (three points in contact). Then, we increased the distance between the contact point and the detector 2.5 and then 10 mm. We kept in contact the two others points when displacing one contact point.

We expressed the influence of positioning the foot in relative error (%). Relative error was the ratio of the absolute value of the difference between proper positioning and with displacement by the value with proper positioning.

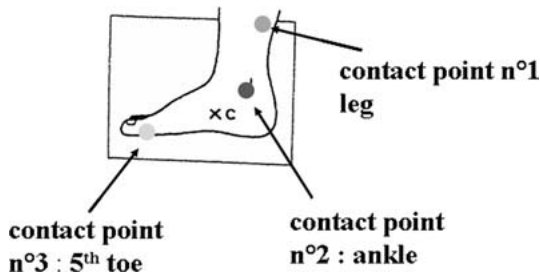


Fig. 5. Schematic representation of the foot with the three points which have to be in contact with the sensor in order to obtain a proper analysis.

Table 1. Reproducibility (CV%) of the bone texture analysis with the three parameters: H_{mean} , run-length, co-occurrence matrices

	H_{mean} (%)	Run-length (%)	Co-occurrence (%)
<i>In vitro</i>	0.25	0.29	0.21
Short-term precision error	1.26	1.24	1.16
Mid-term precision	1.45	0.88	0.84
IntraOR	0.15	0.26	0.17
InterOR	0.39	0.37	0.26
Interprototype comparison	0.90	0.57	0.65

Comparison of Texture Analysis and BMD at the Os Calcis

BMD and texture analysis of the left heel were obtained in 57 females with a mean age of 53.21 ± 9.64 years (range 24–72). BMD measurements were performed using a protocol software on a QDR 1000 from Hologic (Waltham, MA). BMD was obtained in a location that fit with the ROI used in the texture analysis and was of the same surface area. Correlations between BMD and texture parameters were evaluated by determining Pearson correlation coefficients.

Comparative Study of Texture Parameters at the Two Os Calcis

Texture parameters of the left and right os calcis were measured in 13 women aged 22.3 ± 3.5 (range 18–31) years, on the same day for each woman. A paired Student's *t*-test was done to compare values between the left and right os calcis. Correlation within measurements was calculated by the Spearman rank correlation coefficient.

Results

The reproducibility results are reported in Table 1. Short-term precision errors ranged 1.16–1.24% according to the texture parameter. Mid-term precision error was slightly higher than short-term precision for H_{mean} but not for the two other texture parameters.

Comparisons of texture analysis and BMD at the os calcis were performed for 57 women. In addition, among these women, BMD at the lumbar spine, femoral neck, and total hip was obtained for 51 women. There were no significant relationships between texture parameters and

Table 2. Correlation between texture parameters measured at the os calcis and BMD at a site-matched ROI of the os calcis, hip, and lumbar spine

	BMD lumbar spine	BMD neck	BMD total hip	BMD os calcis
H_{mean}				
<i>r</i>	-0.0211	-0.1245	-0.0585	-0.0202
<i>P</i>	0.88	0.38	0.68	0.88
Co-occurrence				
<i>r</i>	-0.1084	-0.2961	-0.1959	0.1766
<i>P</i>	0.45	0.03	0.17	0.19
Run-length				
<i>r</i>	-0.176	-0.3136	-0.2247	0.1295
<i>P</i>	0.22	0.03	0.11	0.34

BMD at a site-matched ROI at the os calcis (Table 2). Furthermore, we did not find any significant relationship between texture parameters at the os calcis and BMD at the lumbar spine. However, we found a mild relationship between the co-occurrence and run-length parameters at the os calcis and BMD at the femoral neck, respectively ($r = 0.29$, $P = 0.03$, and $r = 0.31$, $P = 0.03$) but not between the texture parameters and total hip BMD.

There was no statistical difference between values of H_{mean} obtained after analysis of the dominant and nondominant os calcis: 0.645 ± 0.061 vs. 0.648 ± 0.062 , respectively (P not significant).

Displacements of the contact points with the detector led to relative errors ranging 0.02–1.53% according to the contact point and the parameters studied.

Discussion

These results suggest that this new high-resolution digital X-ray prototype provides better precision data of texture parameters than those found previously [24] on digitized film. The reproducibility of texture parameters with our technique is comparable to the reproducibility of BMD [33, 34], which is the reference technique for bone quantitative measurement.

The better results of reproducibility – e.g., 1.45% vs. 2.07% [24] for mid-term precision error – might be explained by the cut-out of the number of steps used in the assessment of the texture parameters. With this new device, the direct digitization avoids the need for film processing reproducibility and high-resolution film scanning.

The study approach for reproducibility was based on specific recommendations by Glüer et al. [32]. Thus, the short-term and mid-term precision error protocols included, respectively, 30 and 14 subjects (28 and 14 subjects were suggested).

Mid-term precision error estimates the error of measurement over periods of time. It should give the limit of this high-resolution digital X-ray device for monitoring texture parameter changes over a period of time. The mid-term CV of our new device has been evaluated at 1.45% for H_{mean} and $< 1\%$ for run-length and co-occurrence parameters. We do not know yet the biological decrease of texture parameters linked to aging and menopause. However, we have recently reported the difference in texture parameters between patients with established osteoporosis (with fractures) and age-matched controls [35]. The reproducibility in the present study was around three times smaller than the difference observed in our case-control study [35]. Furthermore, if we compare our CV results with the range of values of texture parameters in the same previous study, it is about 14–16 times smaller.

Usually, mid-term precision errors are larger than short-term precision errors. In our study, we found lower mid-term precision errors than short-term precision errors for run-length and co-occurrence parameters. This may be explained in part by the age of subjects included in the short-term precision protocol, which was higher than that in the mid-term precision protocol. Furthermore, health status was different for patients in the short-term protocol and both patients and members of staff in the mid-term protocol.

The positioning of the foot is also a major component of measurement precision as it has been demonstrated both for dual-energy X-ray absorptiometry (DXA) and for ultrasound measurements at the os calcis [35, 36]. For the present technique, the positioning of the heel across the beam along the mediolateral axes of the foot has to be carefully controlled, but the three steps of displacement imparted to the foot phantom in this study led to weak changes (relative error $< 1.5\%$). The contact points, which have to be placed with careful attention, are the ankle and the leg. This is probably explained by the location of the ROI (near the ankle point) and its anatomical marks.

OP is a systemic skeletal disease, but the decrease in bone mass and eventually in microarchitectural deterioration is heterogeneous. It has been shown that OP prevalence is dependent on the measurement site [37]; therefore, the more sites we measure, the more the diagnostic sensitivity improves. Thus, it could be argued, when we assess bone texture parameters at the os calcis to separate osteoporotic women with fracture from controls [17], that this discrimination is linked to the fact that this assessment is made at the os calcis (a third site) in addition to BMD measurements at the lumbar spine and the hip. In this study, we have demonstrated that there was no relationship between the three parameters of texture and BMD assessed at a site-matched ROI at the os calcis (Table 2). This is particularly in accordance with fundamental theory about the

fractal dimension, which is known to be independent of the gray level of images [28]. However, in this study, we found weak correlations between BMD at the femoral neck and the co-occurrence and run-length parameters at the os calcis (Table 2). Our results show that BMD would explain 9% or less of the variance of these texture parameters. These results are also in accordance with a previous study describing the effects of age and time since menopause with the fractal parameter H_{mean} [38]. In this latter study, using radiographic films, 427 women were included and we found a lack of correlation between total hip BMD as well as lumbar spine BMD and H_{mean} ($r = 0.08$, $P = 0.08$, and $r = 0.02$, $P = 0.74$, respectively) and a slight correlation between H_{mean} and femoral neck BMD ($r = 0.13$, $P = 0.008$) [15].

Conclusion

This new high-resolution digital X-ray device enhances the reproducibility of texture parameter measurements versus indirect digitization of radiologic films. Texture parameters measured at the os calcis were not associated with BMD. The reproducibility of this technique compares favorably with DXA precision and allows intergroup comparisons as well as multicenter cross-sectional and prospective studies in fracture risk assessment.

Acknowledgment. This work was made possible by grants from Programme Hospitalier de Recherche Clinique.

References

1. World Health Organization (1994) Assessment of Fracture Risk and Its Application to Screening for Postmenopausal Osteoporosis. Technical Report Series 843. WHO, Geneva
2. Schuit SC, van der Klift M, Weel AE, de Laet CE, Burger H, Seeman E, Hofman A, Uitterlinden AG, van Leeuwen JP, Pols HA (2004) Fracture incidence and association with bone mineral density in elderly men and women: the Rotterdam Study. *Bone* 34:195–202
3. Stone KL, Seeley DG, Lui LY, Cauley JA, Ensrud K, Browner WS, Nevitt MC, Cummings SR (2003) BMD at multiple sites and risk of fracture of multiple types: long-term results from the study of osteoporotic fractures. *J Bone Miner Res* 18:1947–1954
4. Ott SM, Kilcoyne RF, Chesnut CH (1987) Ability of four different techniques of measuring bone mass to diagnose vertebral fractures in postmenopausal women. *J Bone Miner Res* 2:201–210
5. Ammann P, Rizzoli R (2003) Bone strength and its determinants. *Osteoporos Int* 14(suppl 3):S13–S18
6. Seeman E, Delmas P (2006) Bone quality – the material and structural basis of bone strength and fragility. *N Engl J Med* 354:2250–2261
7. Consensus Development Conference (1993) Prophylaxis and treatment of osteoporosis. *Am J Med* 94:646–650
8. Van der Linden JC, Homminga J, Verhaar JAN, Weinans H (2001) Mechanical consequences of bone loss in cancellous bone. *J Bone Miner Res* 16:457–465
9. Lespessailles E, Chappard C, Bonnet N, Benhamou CL (2006) Imaging techniques for evaluating bone microarchitecture. *Joint Bone Spine* 73:254–261

10. Veenland JF, Grashuis JL, Weinans H, Ding M, Vrooman HA (2002) Suitability of texture features to assess changes in trabecular bone architecture. *Pattern Recognition Lett* 23:395–403
11. Majumdar S, Lin J, Link T, Millard J, Augat P, Ouyang X, Newitt D, Gould R, Kothari M, Genant H (1999) Fractal analysis of radiographs: assessment of trabecular bone structure and prediction of elastic modulus and strength. *Med Phys* 26:1330–1340
12. Lin JC, Grampp S, Link T, Kothari M, Newitt DC, Felsenberg D, Majumdar S (1999) Fractal analysis of proximal femur radiographs: correlation with biomechanical properties and bone mineral density. *Osteoporos Int* 9:516–524
13. Link TM, Majumdar S, Konermann W, Meier N, Lin JC, Newitt D, Ouyang X, Peters PE, Genant HK (1997) Texture analysis of direct magnification radiographs of vertebral specimens: correlation with bone mineral density and biomechanical properties. *Acad Radiol* 4:167–176
14. Pothuau L, Benhamou CL, Porion P, Lespessailles E, Harba R, Levitz P (2000) Fractal dimension of trabecular bone projection texture is related to three-dimensional microarchitecture. *J Bone Miner Res* 15:691–699
15. Guggenbuhl P, Bodic F, Hamel L, Baslé MF, Chappard D (2006) Texture analysis of X-ray radiographs of iliac bone is correlated with bone micro-CT. *Osteoporos Int* 17:447–454
16. Luo G, Kinney JH, Kaufman JJ, Haupt D, Chiabrera A, Siffert RS (2000) Relationship between plain radiographic patterns and three-dimensional trabecular architecture. *J Bone Miner Res* 9:339–345
17. Benhamou CL, Poupon S, Lespessailles E, Loiseau S, Jennane R, Siroux V, Ohley W, Pothuau L (2001) Fractal analysis of radiographic trabecular bone texture and bone mineral density: two complementary parameters related to osteoporotic fractures. *J Bone Miner Res* 16:697–704
18. Black DM, Steinbuch M, Palermo L, Dargent-Molina P, Lindsay R, Hoseyni MS, Johnell O (2001) An assessment tool for predicting fracture risk in postmenopausal women. *Osteoporos Int* 12:519–528
19. Dempster D (2000) The contribution of trabecular architecture to cancellous bone quality [editorial]. *J Bone Miner Res* 15:20–23
20. Recker R, Masarachia P, Santora A, Howard T, Chavassieux P, Arlot M, Rodan G, Wehren L, Kimmel D (2005) Trabecular bone microarchitecture after alendronate treatment of osteoporotic women. *Curr Med Res Opin* 21:185–194
21. Borah B, Dufresne TE, Chmielewski PA, Johnson TD, Chines A, Manhart MD (2004) Risedronate preserves bone architecture in postmenopausal women with osteoporosis as measured by three-dimensional microcomputed tomography. *Bone* 34:736–746
22. Jiang Y, Zhao JJ, Mitlak BH, Wang O, Genant HK, Eriksen EF (2003) Recombinant human parathyroid hormone (1–34) (teriparatide) improves both cortical and cancellous bone structure. *J Bone Miner Res* 18:1932–1941
23. Benhamou CL, Chappard C, Gadois C, Lemineur G, Lespessailles E, de Vernejoul MC, Fardellone P, Delmas P, Weryha G, Harba R (2004) Characterization of trabecular micro-architecture improvement under teriparatide by a fractal analysis of texture on calcaneus radiographs. *J Bone Miner Res* 19(suppl 1):S126
24. Benhamou CL, Lespessailles E, Jacquet G, Harba R, Jennane R, Loussot T, Tourliere D, Ohley W (1994) Fractal organization of trabecular bone images on os calcis radiographs. *J Bone Miner Res* 9:1909–1918
25. Lespessailles E, Roux JP, Benhamou CL, Arlot ME, Eynard E, Harba R, Padonou C, Meunier JP (1998) Fractal analysis of bone texture on os calcis radiographs compared with trabecular microarchitecture analyzed by histomorphometry. *Calcif Tissue Int* 63:121–125
26. Lespessailles E, Jullien A, Eynard E, Harba R, Jacquet G, Ildelfonse JP, Ohley W, Benhamou CL (1998) Biomechanical properties of human os calcanei: relationships with bone density and fractal evaluation of bone microarchitecture. *J Biomech* 31:817–824
27. Pothuau L, Lespessailles E, Harba R, Jennane R, Royant V, Eynard E, Benhamou CL (1998) Fractal analysis of trabecular bone texture on radiographs: discriminant value in postmenopausal osteoporosis. *Osteoporos Int* 8:618–625
28. Lundahl T, Ohley WJ, Kay SM, Siffert R (1986) Fractional brownian motion: a maximum likelihood estimator and list application to image texture. *IEEE Trans Med Imaging* 5:152–161
29. Haralick R (1986) Statistical image texture analysis. In: *Handbook of Pattern Recognition and Image Processing*. Academic Press, San Diego, pp 247–279
30. Galloway MM (1975) Texture analysis using gray level run lengths. *Comput Graph Image Proc* 4:172–179
31. Chu A, Sehgal CM, Greenleaf JF (1990) Use of gray value distribution of run lengths for texture analysis. *Pattern Recognition Lett* 11:415–419
32. Glüer CG, Blake G, Lu Y, Blunt BA, Jergas M, Genant HK (1995) Accurate assessment of precision errors: how to measure the reproducibility of bone densitometry techniques. *Osteoporos Int* 5:262–270
33. Economos CD, Nelson NE, Fiatorone MA, Dallal GE, Heymsfield SB, Wang J, Russel-Audet M, Yasumura S, Vaswani AN, Pierson RN (1996) A multicenter comparison of dual energy X-ray absorptiometers: in vivo and in vitro measurements of bone mineral content and density. *J Bone Miner Res* 11:275–285
34. Pouilles JM, Tremollières F, Todorovsky N, Ribot C (1991) Precision and sensitivity of dual-energy X-ray absorptiometry in spinal osteoporosis. *J Bone Miner Res* 6:997–1002
35. Brooke-Wavell K, Jones PRM, Pye DW (1995) Ultrasound and dual X-ray absorptiometry measurement of the os calcis: influence of region of interest location. *Calcif Tissue Int* 57:20–24
36. Evans WD, Jones EA, Owen GM (1995) Factors affecting the in vivo precision of broadband ultrasonic attenuation. *Phys Med Biol* 40:137–151
37. Greenspan SL, Maitland R, Myers E (1996) Classification of osteoporosis in the elderly is dependent on site specific analysis. *Calcif Tissue Int* 58:409–414
38. Lespessailles E, Poupon S, Niamane R, Loiseau-Peres S, Derommelaere G, Harba R, Courteix D, Benhamou CL (2002) Fractal analysis of trabecular bone texture on os calcis radiographs: effects of age, time since menopause and hormone replacement therapy. *Osteoporos Int* 11:366–372